Chalcogenide Letters Vol. 10, No. 8, August 2013, p. 259 - 272

RDE VOLTAMMETRY AND IMPEDANCE SPECTROSCOPY STUDIES OF Sb, Te AND SbTe ELECTRODEPOSITION FROM CHOLINE CHLORIDE – UREA IONIC LIQUIDS

M. L. MARES, F. GOLGOVICI*, T. VISAN
Faculty of Applied Chemistry and Materials Science, University POLITEHNICA of Bucharest,
1-7 Polizu Street, 011061 Bucharest, Romania

The paper presents the investigation of electrode processes during electrodeposition of antinomy, tellurium and antimony telluride on Pt and glassy carbon electrodes from ionic liquids containing a mixture of choline chloride with urea (1:2 mole ratio). $SbCl_3$ and TeO_2 in 2-5 millimolar concentration were introduced as precursors in the supporting electrolyte. Cyclic voltammetry, voltammetry with rotating disk electrode and electrochemical impedance spectroscopy techniques were used at 60^0C to evidence the deposition/dissolution processes on both Pt and glassy carbon electrodes. SbTe induced codeposition takes place on a Te layer which can partial or fully cover the electrode surface. Experimental data suggested that the electrodeposition of Sb and Te elements and SbTe compound are kinetically less favored if glassy carbon electrode is used instead of platinum.

(Received June11, 2013; Accepted August 5, 2013)

Keywords: Electrochemical deposition; Antimony; Tellurium; Antimony telluride; RDE voltammetry; Electrochemical impedance spectroscopy

1. Introduction

Although antimony films have a brittle silvery–white metallic aspect, Sb is also considered a semimetal [1] with an energy overlap (0.18 eV) between the conduction and valence bands at 4.2 K, thus having unusual electronic transport which occurs *via* both electrons and holes. Pure (unalloyed) antimony is not often used in industry, but its alloys and chemical compounds have found wide commercial applications. Antimony is a component of some alloys such as Cu_2Sb, SnSb, AlSb, $CoSb_3$ $ZnSb_3$, InSb and $InAs_{1-x}Sb_x$. Moreover, antimony is a component of many semiconductor compounds with solar cells, humidity sensors and thermoelectrical applications [2-4] such as thermoelectrical generators, thermopile sensors and microcoolers.

One the most used antimony compounds is diantimony tritelluride, Sb_2Te_3, which is a narrow band-gap semiconductor (Eg = 0.3 eV) with a rhombohedral crystal structure and a trigonal symmetry. Like bismuth telluride, Bi_2Te_3, antimony telluride has a large thermoelectric effect and is therefore used in solid state refrigerators. In addition to solar cell devices and thermoelectric applications, Sb_2Te_3 film is considered as a candidate for non-volatile phase change memory devices, replacing $Ge_2Sb_2Te_5$, because of its low melting temperature and ability to reversibly transform between amorphous to crystalline states with high speed [5, 6].

Thin SbTe films may be obtained by many different techniques including thermal evaporation, sputtering, molecular beam epitaxy, metal-organic chemical vapor deposition (MOCVD) or hydrothermal/solvothermal synthesis. The electrodeposition has been also applied to obtain high quality thin films of Sb_2Te_3 semiconductor. There have been a large number of recent published papers [2-15] concerning SbTe films electrodeposition from aqueous electrolytes, in the majority of works acidic solutions (with nitric acid or hydrochloric acid) being used. Compared to other methods, electrodeposition has relatively low cost and therefore may be an efficient method

* Corresponding author: floregov@yahoo.com

to produce thin films. The most interesting feature in electrodeposition is that the composition and crystalline structure of deposited material can be controlled by adjusting the operation parameters. It can be conducted at room temperature, and can be used to fill high aspect ratio geometries that are not accessible by other deposition methods.

However, it is very difficult in aqueous solutions to obtain Sb_xTe_y thin films with a sufficiently high concentration of Sb, especially the composition of Sb_2Te_3 compound, because the Sb(III) ions tend to hydrolyze and precipitate. This limits the maximum deposition rate and causes difficulties in controlling the bath composition. To resolve these difficulties, other non-aqueous liquid media such as organic solvents, molten salts and ionic liquids that are often able to dissolve relatively high concentrations of (semi)metal salts have been introduced. Examples are published papers reporting electrodeposition of antimony [16-21] and antimony compounds [22]. The main advantage consists in a one-step electrodeposition of crystalline Sb_2Te_3 without the need for additional processing. Also a good compositional control is possible using organic media, melts or traditional ionic liquids (imidazolium-based liquids, for instance), but in general these electrolytes are too expensive for practical application.

Recently, Abbott *et al* [23] have described a new ionic liquid based on a deep eutectic consisted in choline chloride (2-hydroxy-ethyl-trimethyl ammonium chloride, **ChCl**) and urea. They demonstrated that urea, and also some amides, glycols or carboxilic acids, are hydrogen bonding donors and the formed eutectic ionic liquids with ChCl consist entirely in two kinds of ions, choline cation and complexed chloride anion. Comparing to other ionic liquids, such media have the additional advantages to be easy to prepare, water and air stable and nontoxic.

Previously, we reported some results regarding the possibility of electrodeposition of Sb and Te as elements or as binary compound using eutectic mixture (1:2 mole ratio) of choline chloride with urea as hydrogen bond donor [24,25]. Also, we have studied the cathodic deposition of other tellurides semiconductors as BiTe and BiSbTe from ChCl-malonic acid [26-28], BiTe and BiTeSe from ChCl-oxalic acid [29, 30], PbTe from ChCl-ethylene glycol [31] and CdTe from ChCl-urea [32] ionic liquids. Stationary Pt electrodes were used in those investigations of electrode processes. We consider that stirring during electrolysis in such viscous media will have a favorable influence to morphology and adherence on substrate of films as well as an increase of productivity in technological applications. Therefore, we have chosen as an investigation tool the voltammetry with rotating disk electrode (RDE) which is more appropriate technique for stirred electrolytes. Electrochemical impedance spectroscopy is also a powerful method of characterizing the electrode processes by changing the deposition potential. We report in this paper the results of studies, on both Pt and glassy carbon disk electrodes, concerning the electrode processes associated to deposition of Sb, Te and Sb_2Te_3 from choline chloride – urea eutectic mixture. To our knowledge processes involving Sb(III) and Te(IV) ions using the rotating electrodes and glassy carbon stationary electrode have not been yet examined or reported in the literature of ChCl containing ionic liquids.

2. Experimental Part

First, a eutectic mixture of 1:2 mole ratio of choline chloride (99%, Aldrich) with urea (Aldrich) was prepared as supporting electrolyte. The appropriate binary mixture was heated at above 90^0C for 30 min until homogeneous colorless ionic liquid is formed. $SbCl_3$ and TeO_2 (both from Alfa Aesar) were used as precursors for the ionic species of antimony and tellurium in ionic liquid. All reagents were used as received. The molarities of solutions were calculated using the density value of ChCl-urea system reported in [33].

Cyclic voltammograms, voltammograms with rotating electrode and electrochemical impedance spectra were recorded using disks with 3 mm diameter, made from Pt and glassy carbon (GC). A Pt plate as auxiliary electrode and a Ag wire (immersed in the same ionic liquid) as quasireference electrode were also used in the electrochemical cell. Rotating disk electrode (RDE) with rotation rates up to 3200 rotations per minute (rpm) is a better tool to evidence the cathodic and anodic processes in stirred electrolyte. The working electrodes were polished with alumina paste, then etched in HNO_3:H_2O 1:1 solution, rinsed and dried before every measurement.

All electrochemical experiments were performed at 60^0C using a Zahner elektrik IM6e potentiostat driven by a PC computer. The voltammograms were recorded at various scan rates from 5 to 200 mVs^{-1}. EIS spectra were obtained with 10 mV a.c. voltage, 100 kHz–100 mHz frequency range, by polarizing cathodic potentials at different values.

3. Results and discussion

By considering the ChCl–urea supporting electrolyte used at 60^0C, we found that the potential window of this electrolyte determined by cyclic voltammetry as a separation between cathodic and anodic limits has values of 2.1-2.2 V for Pt electrode and 3.08-3.13 V for GC electrode, depending on the potential scan rate. $SbCl_3$ dissolved in the ChCl-urea ionic liquid to form colourless or whitish colour solutions for concentrations up to 2-3 M. TeO_2 has a greater solubility in ChCl-urea allowing us to carry out the work even with more than 10 mM concentration [24,25]. To establish the deposition potentials of Sb, Te, and SbTe compound we evaluated at 60^0C the electrochemical behaviors of Sb(III) and Te(IV) ions in the ChCl-urea (1:2 mole ratio) ionic liquid by three techniques: cyclic voltammetry (CV), voltammetry with rotating disk electrode and electrochemical impedance spectroscopy. It is worth to mention that RDE voltammetry and glasyy carbon electrodes used in this paper are presented for the first time in literature of synthesis of chalcogenide compounds in ionic liquids.

3.1. Electrode processes of single Sb(III) ions

Figure 1 shows comparatively families of CV curves exhibiting deposition and dissolution processes in choline chloride – urea + 2mM Sb(III) on platinum disk electrode as a stationary electrode (Fig. 1a) and rotating electrode (Fig. 1b).

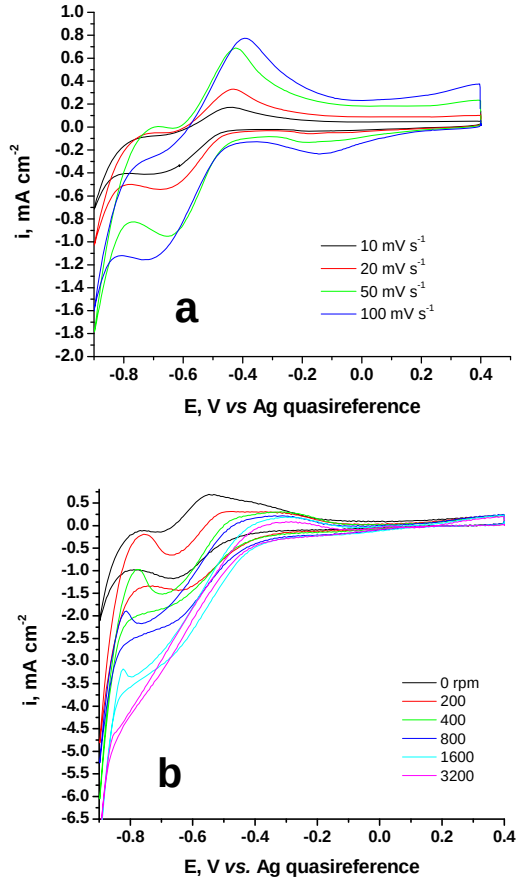

Fig. 1. CVs obtained from ChCl-urea + 2mM $SbCl_3$ ionic liquid at 60^0C: (a) stationary Pt electrode at various scan rates (mVs^{-1}); (b) RDE Pt electrode at various rotation rates (rpm), 50mVs^{-1}

During recording typical cyclic voltammogram, the potential was scanned in the negative direction up to -1.1V and reversed positively until +0.5 V where the second reversal of potential is carried out. In Fig. 1a, a single couple of reduction/oxidation peaks is recorded with peaks centered at *ca.* -0.64V and -0.4 V, respectively. We notice that the amplitudes of peaks (current density i_p) increase with scan rate suggesting a diffusion controlled process. From the linear dependence of cathodic peak current density with square root of scan rate an estimation of diffusion coefficient (D) for Sb(III) ions can be made using the well-known Randles-Sevcik, as a quantitative evaluation. An obtained value of 1.19×10^{-6} cm^2s^{-1} at 60^0C is in a good agreement with previous data reported by us in ChCl-urea at higher temperatures [24]. It is worth to mention that the second cathodic peak that occurred at -0.1V, before the main peak of Sb bulk deposition, may be assigned to underpotential deposition (UPD) of antimony. This process is a surface-limited reaction of Sb atoms deposited on the inert Pt substrate, with a partial covering of the electrode surface. UPD process takes place at more positive potentials than the deposition equilibrium potential (Nernst potential). UPD involves deposition onto naked substrate while bulk deposit growth takes place onto a substrate surface modified by an atomic layer, which was formed during the UPD process.

Regarding the influence of rotation rate of Pt disk on the shape of CVs (Fig. 1b) a gradual change in shape of cathodic portions of antimony deposition is observed, from a peak to a plateau (or shoulder) of limiting current density i_L. Fig. 1b illustrates an increased i_L value with rotation rate, with a dependence which seems to obey the Levich equation valid for mass transport controlled process:

$$i_L = 0.62\, n\, F\, D^{2/3}\, \nu^{-1/6}\, \omega^{1/2}\, c \qquad (1)$$

where ν is the kinematic viscosity (cm^2s^{-1}), ω is the angular velocity ($2\pi\times v_{rot}$, s^{-1}) computted from rotation rate v_{rot} (rms), and n, F and c are the number of electrons in the electrode process, Faraday constant and Sb(III) ion concentration, respectively.

Also, Fig. 1b indicates a gradual shift of cathodic potential with rotation rate, starting from -0.64 V. Higher rotation rates have led to more negative potentials of peaks or plateaus suggesting a degree of ireversibility of cathodic process. Regarding the anodic peak of Sb dissolution its peak potential and peak current are strongly influenced by occurrence of a new oxidation peak before it. This supplementary anodic process is certainly the oxidation of some quantitites of products resulted by reduction of choline cation at more negative potentials than -0.9V.

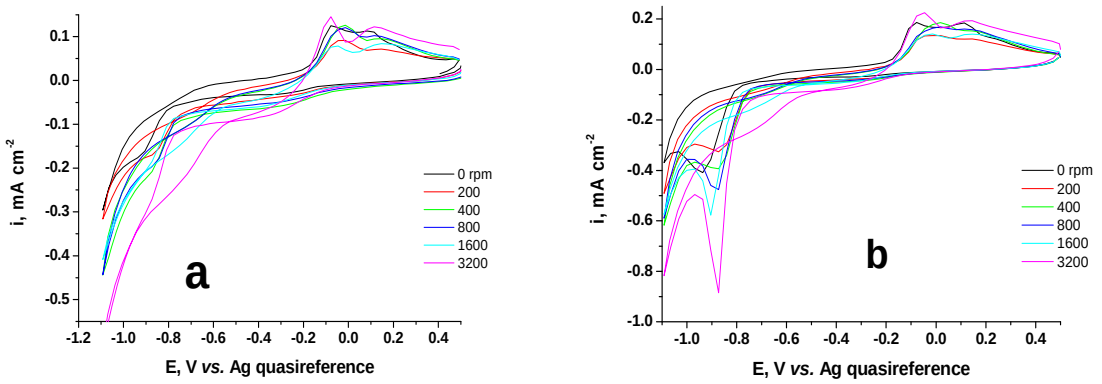

Fig. 2. Influence of cycling to CVs on RDE GC electrode from ChCl-urea + 5mM $SbCl_3$ system, 60^0C, $50mVs^{-1}$: (a) first cycle; (b) second cycle.

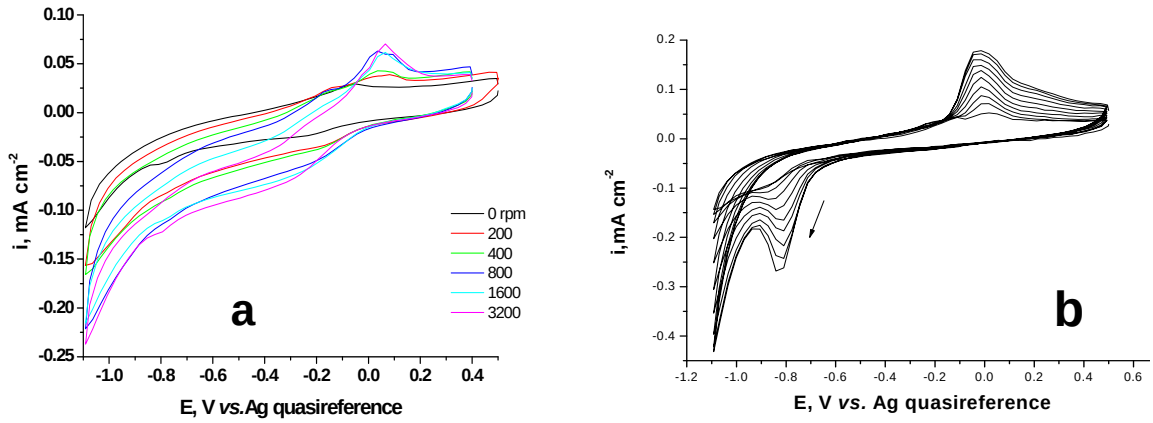

Fig. 3. CVs on RDE GC electrode recorded from ChCl-urea + 2mM $SbCl_3$ system, 60^0C, $50mVs^{-1}$: (a) first cycle; (b) 10 cycles of repetitive CVs on stationary GC electrode (0 rpm)

A quite similar shape of RDE voltammograms is found using glassy carbon (Figs. 2 and 3) instead of platinum electrode. Fig. 2a and Fig. 2b present the difference between two families of CVs recorded in 5mM Sb(III) solution, which consists in different shape of cathodic branch. Thus, a plateau or a shoulder in the potential region from -0.5V to -0.8V in the first cycle (Fig. 2a) and a prominent reduction peak (at around -0.87V) in the second one (Fig. 2b) are observed. Similar shape as in Fig. 2a was obtained for cathodic branches in the first scanning using 2mM Sb(III) solution (

Fig. 3a), but now the process starts at more positive potentials, at *ca.* -0.3V. The amplitude of reduction peak increases by continuing the cycling, 10 repetitive cycles, for instance in

Fig. 3b. The cathodic current density increases with rotation rate and with Sb(III) concentration proving the existence of mass transport control for GC electrode, too. More complicated is the shape of anodic peaks in these Figures. The shape of 'twins' may be due to a superposition of two consecutive anodic processes: the first process is the oxidation of products formed additionally onto GC surface during scanning along reduction branch at very negative potentials and the second one is dissolution of Sb deposit which is stripped from GC surface.

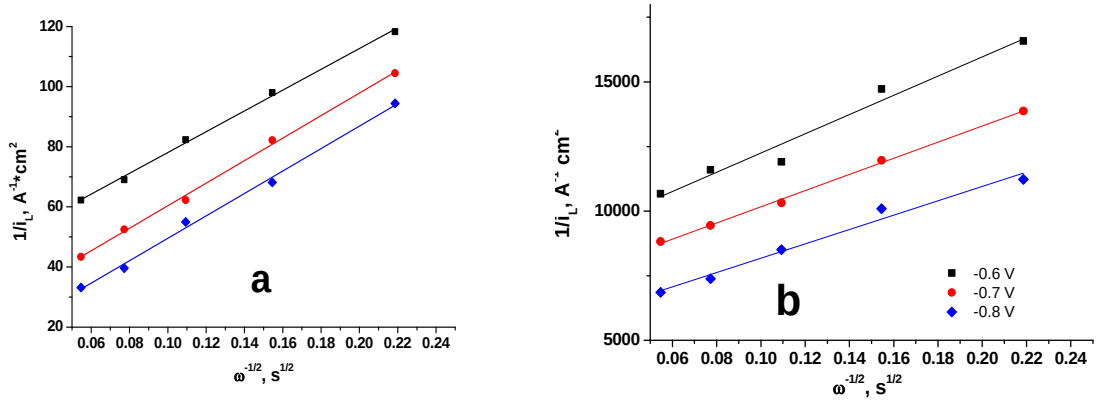

Fig. 4. Koutecky-Levich plots corresponding to cathodic limiting currents determined at various potentials from CVs recorded in ChCl-urea + 2mM $SbCl_3$ systems, 60^0C, $50mVs^{-1}$: (a) RDE Pt electrode; (b) RDE GC electrode.

Even though the Sb(III) electroreduction process is not complicated by other competitive reactions, the assumption of a simple mass transport control (diffusive and convective transport) is not realistic. From this reason, a modified form of Levich equation valid for mixed control (activation and mass-transport) may be utilized. Plots of the reciprocal RDE current densities

against reciprocal square root of angular velocity, constructed from data taken at potentials of the plateau (or shoulder) on RDE voltammograms, were linear and quite parallel (Fig. 4), indicating a Levich behaviour according to equation (2) valid for kinetic complication:

$$\frac{1}{i_L} = \frac{1}{i_k} + \frac{1}{0.62\, n F\, D^{2/3}\, c\, \nu^{-1/6}\, \omega^{1/2}} \tag{2}$$

where i_k is the activation-controlled current density, denoted also as kinetic current density i_k or current density under pure kinetic control. The different intercepts with ordinate axis of parallel straightlines in Figures 4a and 4b show that pure activation-controlled current density has a clear dependence on the applied potential and chemical nature of the electrode.

The cathodic formation of Sb films was also studied by the electrochemical impedance spectroscopy measurements at 60^0C.

Fig. 5 and Fig. 6 present the impedance spectra obtained from electrolytes containing 2mM and 5mM $SbCl_3$. In

Fig. 5 Nyquist diagram shows the dependence of imaginary part of impedance vs. real part of impedance, whereas Bode diagram represents simultaneously two dependences: impedance modulus *vs*. frequency and phase angle *vs*. frequency.

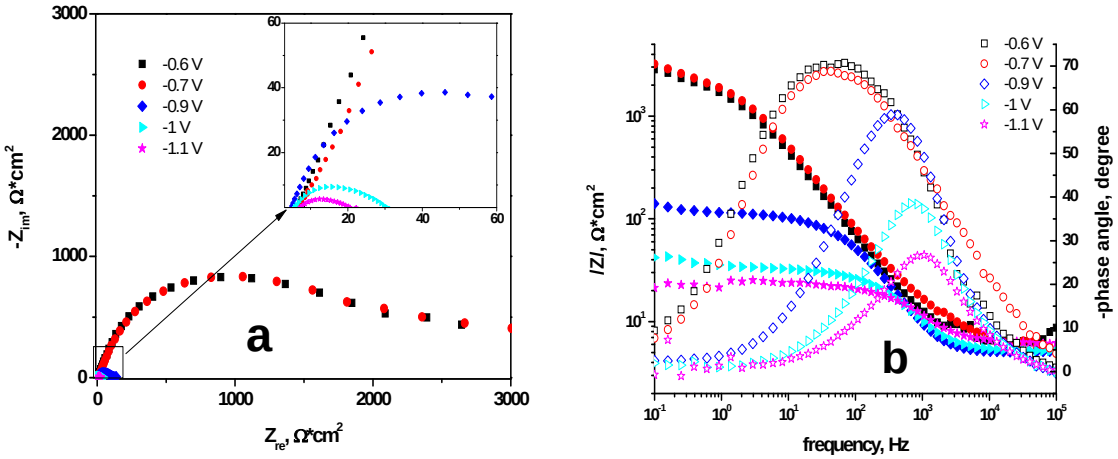

Fig. 5. Nyquist (a) and Bode (b) diagrams on Pt electrode from ChCl-urea + 2mM $SbCl_3$ system, 60^0C, at various polarization potentials.

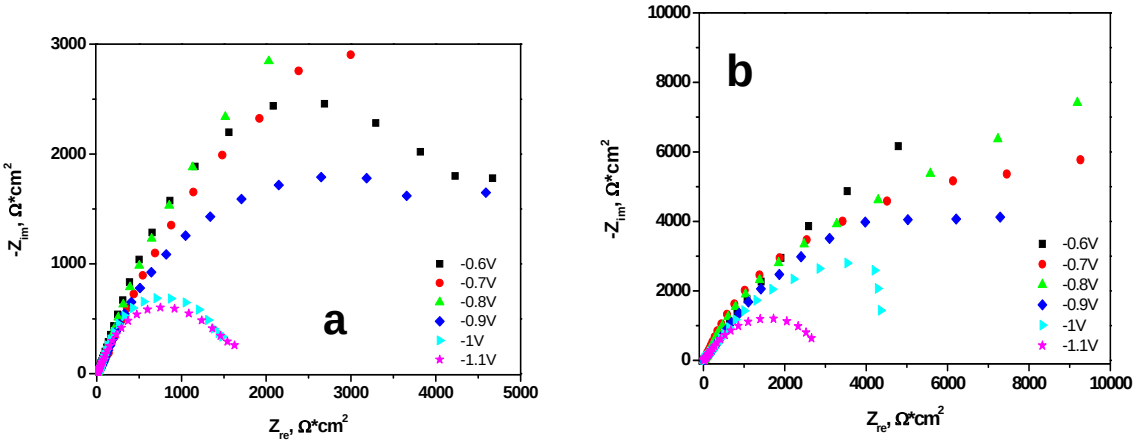

Fig. 6. Nyquist diagrams recorded at various polarization potentials on GC electrode from ChCl-urea ionic liquid with two concentrations of $SbCl_3$, 60^0C: (a) 5mM $SbCl_3$; (b) 2mM $SbCl_3$.

The electrode was gradually polarized in the potential region where the reduction process has a significant cathodic current (peak or limiting current) on CV curves. Thus, the impedance results are interpreted in relation with voltammetric results. At polarization of -0.6V and -0.7V the capacitive semicircle located at high frequencies continues within low frequency region with a straightline indicating the formation of Sb film onto the Pt electrode surface. This corresponds to deposition at potentials around peak potential in CV curves or within limiting current range in RDE voltammograms. For more negative polarization a gradual decrease of the semicircle diameter is observed, from 2300Ωcm^2 to 20 Ωcm^2, which means a continuous increase of current density when several Sb layers are deposited on platinum electrode. Corespondingly, Bode diagram shows a continuous decrease of negative phase angle which is changed progressively from -68^0 to -26^0 proving the metallic character of deposit.

Similar interpretation can be presented for impedance spectra recorded on glassy carbon electrode immersed in solutions with Sb(III) concentrations of either 5mM (Fig. 6a) or 2mM (Fig. 6b). By polarizing the carbon electrode from -0.6V to -1.1V, the diameter of semicircles decreases in the limits of 10000-1600Ωcm^2 for concentrated solution and 20000-3000Ωcm^2 for diluted solution. Comparative with platinum electrode the semicircle diameters for GC substrate are with one order of magnitude smaller. This is a good illustration of the difference in the electrolysis current, leading to the recommendation that in technological conditions high deposition rates will be obtained in concentrated solutions and suitable electrodes.

3.2. Electrode processes of single Te(IV) ions

Tellurium is a semiconductor with energy gap band of 0.4 eV, but tellurium films have good electrical conductivity at room temperature. The great interest in investigation the cathodic reduction of Te(IV) ion onto different substrates is justified owing to numerous applications of tellurides films. The kinetics of tellurium ion was extensively investigated using stationary electrodes in aqueous solutions in relation to synthesis of Sb_2Te_3 films or other telluride films [3]. Also, researches regarding nature of processes involving Te(IV) ion in organic media [34, 35] and molten mixtures [19, 21, 36] were reported. We published in several previous papers [24, 25, 32] the results of cyclic voltammetry and impedance spectroscopy using ChCl-urea ionic liquid with a content of 0.1-10mM TeO_2 and stationary Pt plate electrodes. In addition to previous determinations we present comparatively in Figures 7-9 RDE voltammograms and impedance spectra for platinum and glassy carbon disk electrodes immersed in ChCl-urea + 5mM TeO_2 at 60^{0}C constant temperature.

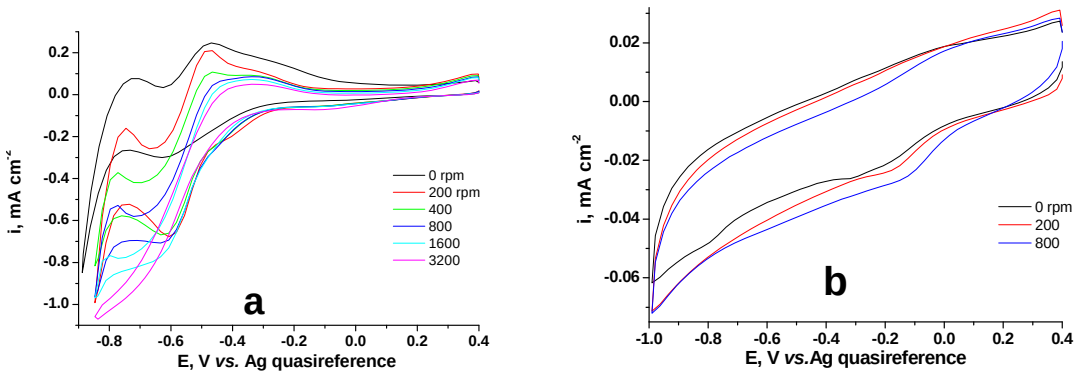

Fig. 7. Comparative CVs with 50mVs^{-1} scan rate from ChCl-urea + 5mM TeO_2 system at 60^{0}C: RDE Pt electrode; (b) RDE GC electrode

Fig. 7a shows that along the RDE voltammetric curves at 60^{0}C on Pt rotating electrode the main reduction process with Te film formation is represented by a peak (at around -0.6V), *e.g.* for 0; 200; 400 rpm, or a plateau at higher rotation rates, 800 and 1600 rpm. The limiting currents of this bulk deposition are recorded if the negative polarization starts from -0.5V and continues up to

-0.9V and more. At these very negative potentials a second process is carried out supplementary, which may be a further reduction of atomic tellurium or, more probably, the reduction of choline cation. However, a less visible reduction process due to underpotential deposition (UPD) of tellurium takes place from 0 to -0.2V in the most positive potential region of cathodic branch. On the anodic branch of RDE voltammograms the coupled anodic peak corresponding to the stripping of Te deposit is located at potentials around -0.5V (Fig. 7a). It can be observed that this peak is accompanied before by an additional anodic peak due to oxidation of fresh products resulting from previous supplementary reduction.

Selected RDE voltammograms in Figure 7b are recorded in the same potential limits as in Fig. 7a in order to have a comparison of Te(IV) ion behaviour on both Pt and GC substrates. Certainly, a quite different shape of cathodic branch of voltammogram is obtained, with a non-pronounced shoulder of limiting current densities (i_L) in a large domain of potentials, from 0V to -0.8V. This wider potential range suggests a mixed reduction process consisting in both UPD and bulk deposition of tellurium atoms on glossy substrate, with a higher percentage of UPD. This is in a good agreement with previous publications [3,12] in which authors stated that almost always UPD cathodic process is involved in the electrodeposition of elementary tellurium. It seems that, unlike CVs for Pt electrode, the participation of choline ion solvent in reduction process on GC electrode is totally absent up to -1V polarization. Regarding the anodic processes, Fig. 7b shows a non-finished oxidation process by scanning the potential up to +0.4V, the anodic peak being probably at more positive potentials.

In support of a good reversibility of tellurium ion behaviour, Figures 7 do not evidenced a shift of peak potential or plateau limit if scan rate increases. Also, in Figure 7a the peak potential separation ΔE_p between the anodic and cathodic peaks has values of maximum 100mV at 60^0C which prove a quite reversible process from electrochemical point of view. Although a quantitative analysis was not performed Figures 7a and 7b illustrate an increased i_L value with rotation rate, according to a dependence which is possible to obey the Levich equation for mass transport control (eq. 1) and suitable for Koutecky-Levich plotting.

In Figures 8 and 9 Nyquist and Bode spectra regarding tellurium deposition were recorded in the same manner as for Sb deposition, *i.e.* by measuring the impedance components during gradual cathodic polarization from stationary potential. Nyquist diagrams show clearly sequences with a single capacitive semicircle for both Pt and GC electrodes. However, only for platinum substrate this capacitive loop is continued at low frequencies with a linear portion (Figure 8), that may be related to formation of a Te deposit within the active Te(IV) species may diffuse toward platinum. For Pt electrode the semicircle diameter decreases with polarization from about 850Ωcm^2 to 200Ωcm^2 indicating a gradual increase of cathodic process rate. The semicircles recorded with glassy carbon substrate (Figure 9) have larger diameters than on platinum, with around one order of magnitude higher at each polarization potential.

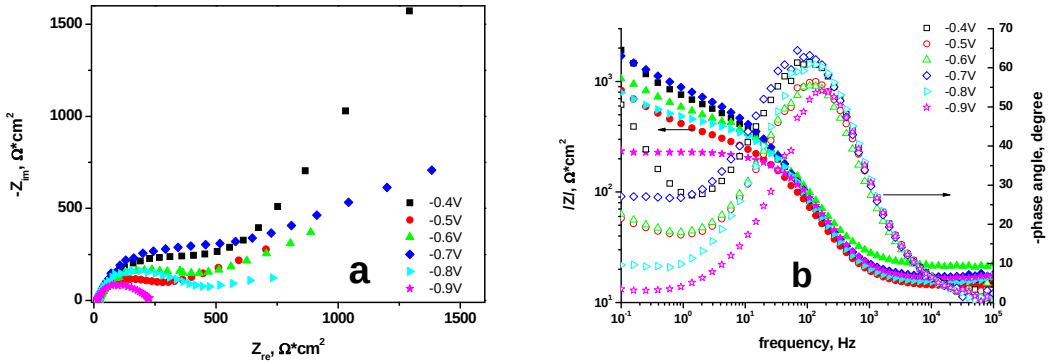

Fig. 8. Nyquist (a) and Bode (b) diagrams on Pt electrode from ChCl-urea + 5mM TeO_2, 60^0C, at various polarization potentials.

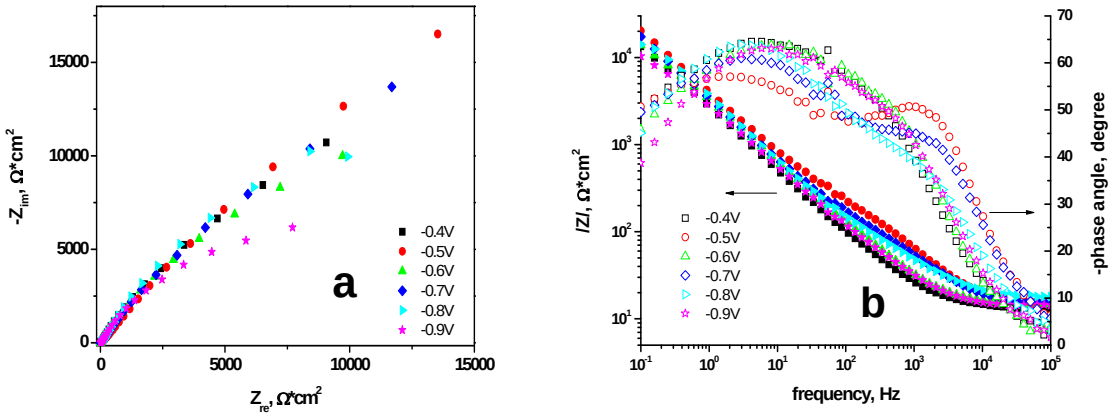

Fig. 9. Nyquist (a) and Bode (b) diagrams on GC electrode from ChCl-urea + 5mM TeO_2, 60^0C at various polarization potentials.

It can be seen in Bode diagrams of Figures 8b and 9b that the maximum of phase angle decreases gradually from -65^0 to -50^0, but this last value does not indicated a metallic behavior of Te deposit. Dependences of impedance modulus with frequency present also a gradual decrease of impedance, confirming the enhancement of tellurium deposition.

3.3. Investigations of solutions containing both Sb(III) and Te(IV) ions

We present in this section the investigation at 60^0C of two ionic liquids containing ChCl–urea (1:2) mixture with different mole ratios between Sb(III) and Te(IV) ions, namely 2mM + 5mM (Figures 10 and 11) and 2mM + 5mM (Figures 12-14), respectively.

Typical CVs recorded at stationary Pt disk for the electrolyte with 2mM Sb(III) and 5mM Te(IV) in ChCl–urea ionic liquid are shown in Figure 10a. On the cathodic scan, we found out a series of consecutive processes represented first by a broad peak in the most positive region (centered at -0.15V), then the main reduction peak which can be associated to SbTe compound formation and finally a continuous increase of current at very negative polarization. On the reverse scan, each CV curve exhibits the anodic peak corresponding to dissolution of SbTe deposit and before it the less pronounced peak of fresh products formed previously during reduction of choline ion solvent at most negative potentials. Typical RDE voltammograms recorded at rotating Pt disk for the same electrolyte are presented in Fig. 10b. Their interpretation is similar with Figure 10a (notice that curve at 0 rms rotation rate is in fact identical to CV curve at $50mVs^{-1}$ from Figure 10a).

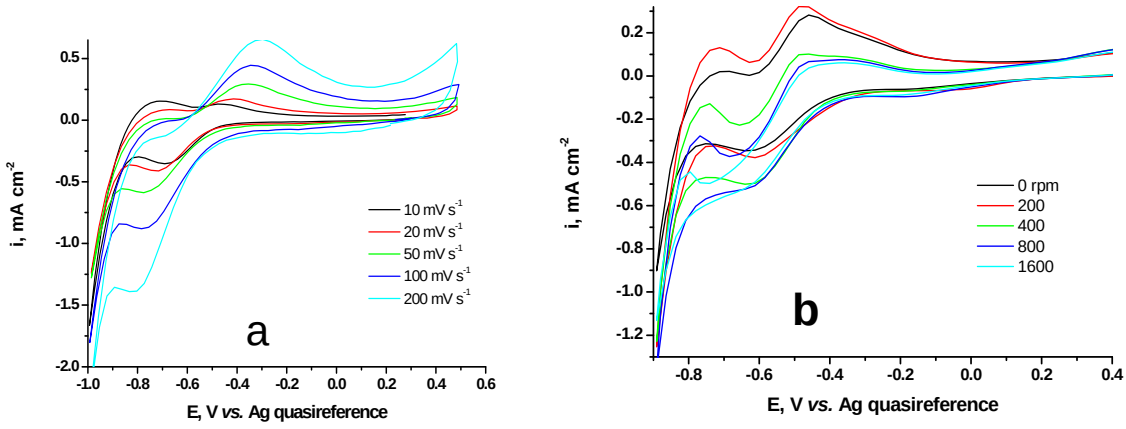

Fig. 10. CVs for deposition of SbTe compound from ChCl-urea + 2mM $SbCl_3$ + 5mM TeO_2 system at 60^0C, $50mVs^{-1}$: (a) stationary Pt electrode at various scan rates (mVs^{-1}); (b) RDE Pt electrode at various rotation rates (rpm)

According to the characteristic electrode potentials of processes exhibited in CV and RDE voltammetry experiments with single ions, we attribute the first cathodic process in Fig. 10a to UPD of a direct discharge to elementary tellurium; it is not clear evidenced, being ill-defined using rotating electrode, similar to RDE curves for systems containing single Te(IV) ion (Figure 7b). The peak corresponding to massive codeposition of Sb and Te is located in the ranges from -0.65V to -0.75V for stationary Pt electrode and from -0.4V to -0.75V for rotating Pt electrode. Actually, in Fig. 10b the peak becomes a plateau of limiting current at higher rotation rates. The increase of peak current density with scan rate (Figure 10a) suggests a diffusion control, whereas the increase of peak (or limiting) current density with rotation rate (Figure 10b) suggests a mixed (diffusion and convection) mass transport control. The cathodic process of SbTe deposition also shifts its peak potential to more negative values if either scan rate or rotation rate increases. Correspondingly, it is noticed on anodic branch the shift of anodic peak potential to more positive values. This behaviour suggests rather a quasi-reversible deposition/dissolution response of Sb and Te codeposition, with a degree of irreversibility due to a slow charge-transfer reaction and/or a possible overpotential required nucleation, especially onto GC electrode surface.

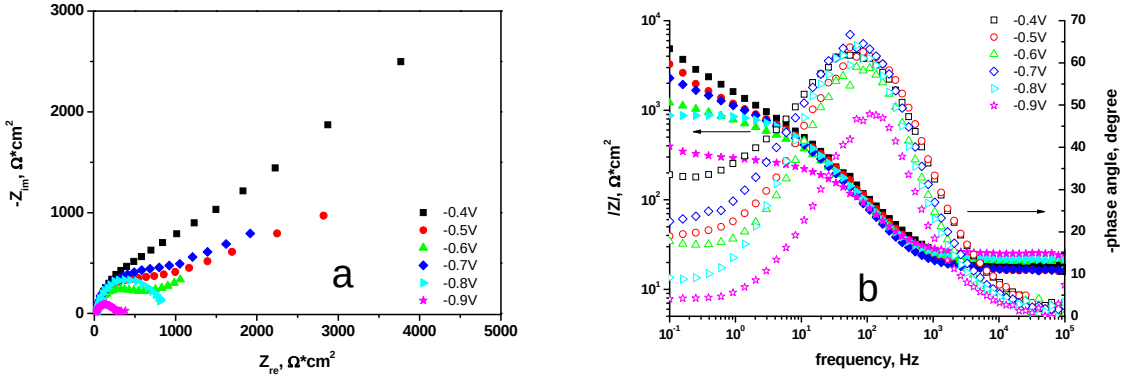

Fig. 11. Nyquist (a) and Bode (b) diagrams on Pt electrode from ChCl-urea + 2mM $SbCl_3$ + 5mM TeO_2 system, 60^{0}C, at various polarization potentials

We suppose that the codeposition process of SbTe in ChCl-urea containing electrolyte can be described, similar to BiTe formation [37], by the general reaction:

$$x\ Sb^{3+} + yTe^{4+} + (3x + 4y)\ e^- \rightarrow Sb_xTe_y \qquad (3)$$

The induced codeposition of SbTe may be favourized in ChCl-urea ionic liquid because it seems for the reduction potentials of antimony and tellurium ions to be closed to each other. The SbTe codeposition process takes place onto a Te layer deposited initially on the substrate. Of course, the particular reaction for the case of Sb_2Te_3 compound formation involves participation of 18 electrons in the reduction process (eq. 3).

All Nyquist spectra displayed in Fig. 11a show usual impedance behaviour of deposition processes with a capacitive semicircle at high frequencies and linear portion at low frequencies. Nyquist curve at -0.4V indicates the start of UPD Te, with a semicircle diameter of 5000Ωcm^2. The process is intensified up to -0.6V (curves with tendency of smaller diameters, 2000 Ωcm^2, 1000 Ωcm^2). Exploring the potential more negatively SbTe formation by massive deposition is evidenced from the Nyquist curves at -0.7V, -0.8V and -0.9V, where diameters from 1500 Ωcm^2 to 200 Ωcm^2 are obtained. SbTe semiconductor formation is also suggested by Bode spectra (Fig. 11b) because the maximum phase angle decreases from -65^0 to less than -50^0.

Cyclic voltammograms at 60^{0}C for 2mM Sb(III) + 2mM Te(IV) systems where also both precursors are jointly dissolved in ChCl-urea are presented in Figs. 12 and 13. Figure 12a gives an example of CV curve recorded on stationary Pt electrode by scanning the electrode potential within a large potential domain. A single couple of deposition/dissolution processes is also clearly

evidenced in Figs. 12b and 12c showing that SbTe deposits are oxidizable by a reverse scan. However, although it is expected for this electrolyte less rich in Te ions (2mM TeO_2 instead of 5mM) the voltammograms to have much lower peak currents, only a small diminish of peak current density is observed; the same is noted for the anodic dissolution peaks as well. This may be explained that fixed stoichiometry of SbTe deposit requires a certain mole ratio in concentration of ions in electrolyte; an exces of Te(IV) may lead to an intensive Te formation as first layers onto platinum electrode but not an intensive SbTe codeposition.

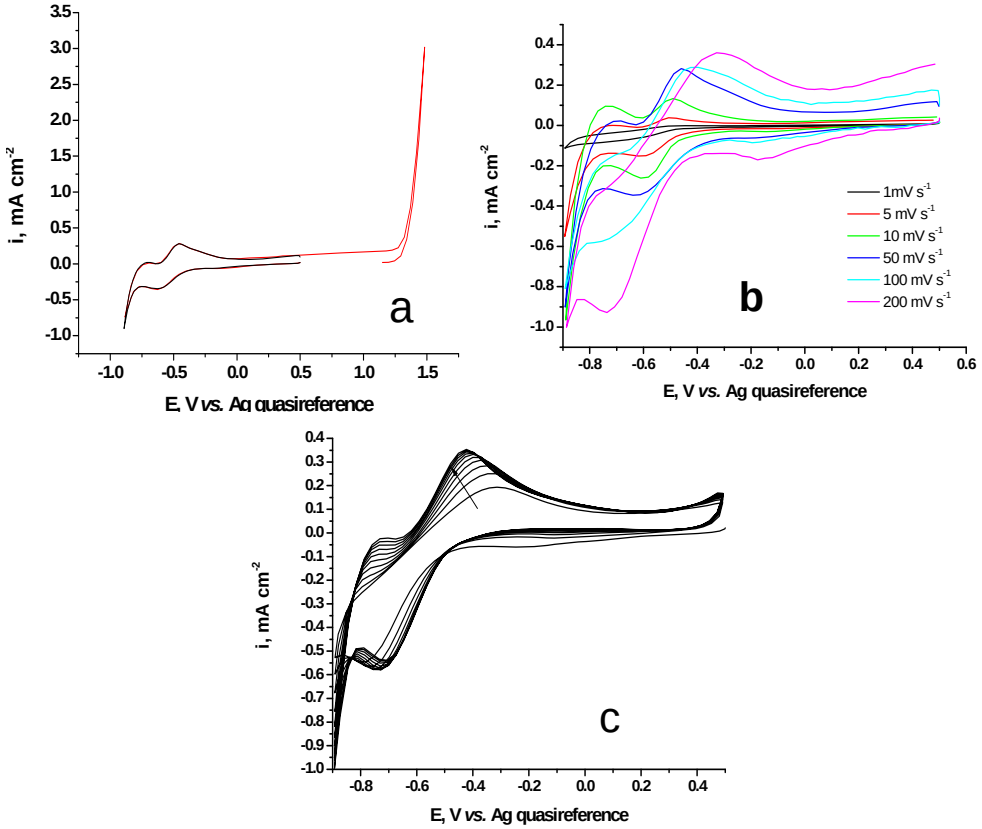

Fig. 12. CVs on stationary Pt electrode for deposition of SbTe compound from ChCl-urea + 2mM $SbCl_3$ + 2mM TeO_2 system at 60^0C: (a) 20mVs^{-1} scan rate; (b) various scan rates: (c) repetitive CVs for the first 10 cycles, 50mVs^{-1}scan rate .

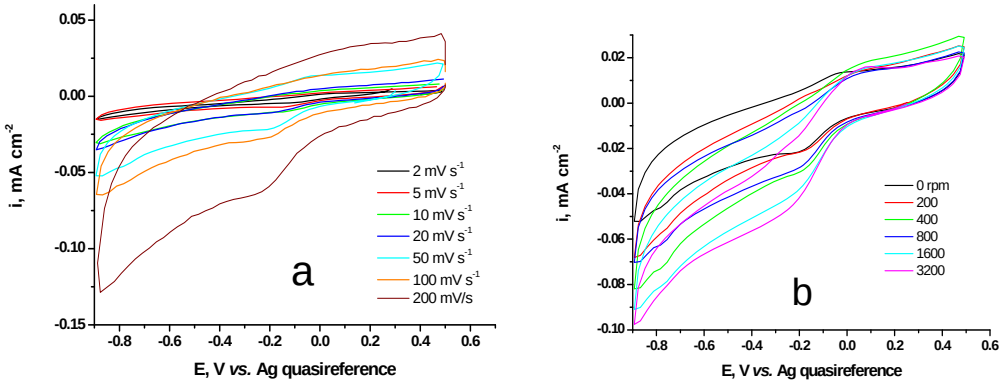

Fig. 13. CVs on GC electrode for deposition of SbTe compound from ChCl-urea + 2mM $SbCl_3$ + 2mM TeO_2 system at 60^0C: (a) stationary GC electrode with various scan rates; (b) RDE GC electrode, 20mVs^{-1} scan rate

Figs. 13 show dramatical changes in the shape and magnitude of the peaks (or shoulders) using GC electrode comparing to Pt electrode. First one may observe an ill-evidenced UPD Te process onto glassy carbon surface. Regarding SbTe codeposition, voltammetric curves on both non-rotating and rotating disk GC electrodes have a shape of limiting currents as plateaus or shoulders that start from a potential value of -0.2V and finish at -0.8V in almost all cases. The overall process on the cathodic branch may be attributed to a mixture of consecutive processes leading to UPD Te, massive Te deposition and massive BiTe deposition. Like voltammetric curves on GC electrode in ChCl-urea + 5mM TeO_2 discussed above, on the anodic branch some non-finished oxidation processes were observed up to +0.5V, the anodic peak being probably at more positive potentials. In all CVs of Figures 12a, 12b and 13a the increase of peak current density with scan rate indicates a diffusion control, whereas the increase of limiting current density with rotation rate (Figure 13b) is related to a mixed (diffusion and convection) mass transport control.

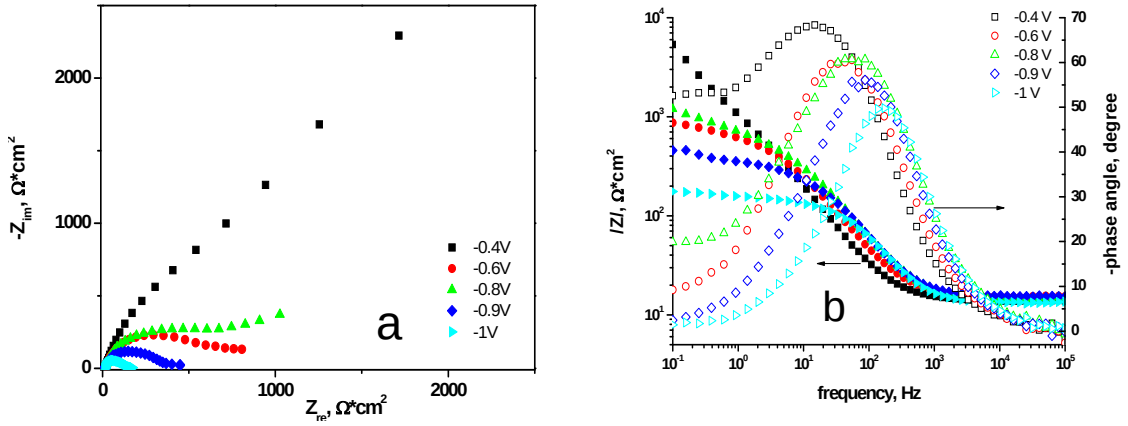

Fig. 14. Nyquist diagrams for deposition of SbTe compound from ChCl-urea + 2mM $SbCl_3$ + 2mM TeO_2 system at 60^0C and various polarization potentials of Pt electrode

The impedance spectra (Nyquist and Bode) obtained on Pt electrode in ChCl-urea + 2mM $SbCl_3$ + 2mM TeO_2 system (Figure 14) are quite similar with impedance spectra from ChCl-urea + 2mM $SbCl_3$ + 5mM TeO_2 system. Thus, in Figure 14a Nyquist curves at -0.4V and -0.6V suggest that UPD Te and massive Te deposition prevails, whereas curves at more negative polarization -0.8V, -0.9V and -1V correspond to a process where only SbTe codeposition is carried out. The semicircle diameters and therefore the electrolysis currents are approximately of the same order of magnitude as for ChCl-urea + 2mM $SbCl_3$ + 2mM TeO_2 system, confirming similar voltammetric data. The formation of SbTe compound having semiconductor characteristics is also suggested by Bode spectra (Figure 14b) where the maximum phase angle decreases from -70^0 to -50^0.

As a comparison of voltammograms from the two electrolytes based on ChCl-urea containing both Sb and Te ionic species, the cathodic peak attributed to SbTe codeposition from 2mM Sb(III) + 5mM Te(IV) system is located approximately in the same potential range as peak values for reduction of a single Sb ion (-0.64V) or single Te ion (-0.6V). However, SbTe formation occurs in 2mM + 2mM system at more negative potentials, at around -0.8V. This different behaviour may be an evidence of the important role played by tellurium ion concentration during the codeposition process. An excess of tellurium ion concentration (1:2.5 mole ratio in investigated solution) leads to an intense UPD Te or/and massive Te deposition; thus the SbTe induced codeposition on a Te layer which completes the whole surface of electrode is kinetically favored. Codeposition of SbTe from a 1:1 mole ratio solution onto an incomplete coverage with Te of the surface may requires more negative potentials to takes place.

In support of this discussion about an increased overpotential for SbTe codeposition in diluted tellurium solutions is a comparison of impedance spectra obtained from investigated systems with both ions. It can be seen comparing Figures 11a and 14a that during polarization at -0.6V the linear tail of Nyquist semicircles is longer for 2mM + 5mM system than for 2mM +2mM

system, meaning that a significant amount of SbTe was deposited. Nyquist curves recorded at higher negative polarizations (-0.8V) are exactly the reverse, with semicircles followed with longer linear portion for 2mM + 2mM system.

4. Conclusions

Studies of cathodic processes from choline chloride – urea eutectic ionic liquids with either single ionic species of Sb(III) and Te(IV) or with both ions were carried out using Pt and glassy carbon disks as stationary or rotating electrodes. Cyclic voltammograms, RDE voltammograms and impedance spectra evidenced for systems with a single ion a couple of cathodic/anodic peaks attributed to reduction/oxidation of elemental antimony or tellurium, respectively. A electroreduction process by underpotential deposition (UPD) that takes place before the bulk (massive) deposition was also revealed for each ion.

The increase of peak current density with scan rate in cyclic voltammograms indicates a diffusion control, whereas the increase of limiting current density with rotation rate in RDE voltammograms is related to a mixed (diffusion and convection) mass transport control. The nature of the electrode is found to have a marked influence on the reduction potentials. Experimental data suggested that the electrodeposition of Sb and Te elements and SbTe compound are kinetically less favored if glassy carbon electrode is used instead of platinum.

Using Pt electrode, the cathodic peak attributed to SbTe codeposition from system with 1:2.5 mole ratio of Sb:Te is located approximately in the same potential range as peak values for reduction of a single Sb ion or single Te ion. However, SbTe formation occurs in system with 1:1 mole ratio of Sb:Te at more negative potentials. An explanation may be that the SbTe induced codeposition takes place on a Te layer which can partial or fully cover the electrode surface. Codeposition of SbTe from a 1:1 mole ratio solution proceeds onto an incomplete coverage of the surface and this may requires more negative potentials.

Acknowledgements

One of the authors recognizes financial support from the European Social Fund through POSDRU/107/1.5/S/76813 Project.

References

[1] Y. Chen, Y. Yang, X. Chen, F. Liu, T. Xie, Mater. Chem. Phys. **126**, 386 (2011).
[2] G. Leimkuehler, I. Kerkamm, R. Reineke-Koch, J. Electrochem. Soc. **149** (1), 474 (2002).
[3] F. Xiao, C. Hangarter, B. Yoo, Y. Rheem, K-H. Lee, N.V. Myung, Electrochim. Acta **53**, 8103 (2008).
[4] M.Y. Kim, T.S. Oh, Surf. Rev. Lett. **17**, 311 (2010).
[5] H. Jung, N.V. Myung, Electrochim. Acta **56**, 5611 (2011).
[6] M.Y. Kim, T.S. Oh, Thin Solid Films **518** (22), 6550 (2010).
[7] D. Del Frari, S. Diliberto, N. Stein, C. Boulanger, J.M. Lecuire, Thin Solid Films **483**, 44 (2005).
[8] C.F.Wang, Q.Wang, L.D. Chen, X.C. Xu, Q. Yao, Electrochem. Solid State Lett. **9**, C147 (2006).
[9] S.K. Lim, M.Y. Kim, T.S. Oh, Thin Solid Films **517** (17), 4199 (2009).
[10] K. Park, F. Xiao, B.Y. Yoo, Y. Rheem, N.V. Myung, J. Alloys Comp. **485**, 362 (2009).
[11] M.Y. Kim, T.S. Oh, J. Electron. Mater. **40** (5), 759 (2011).
[12] J.H. Lim, M.Y. Park, D.C. Lim, B. Yoo, J.H. Lee, N.V. Myung, K.H. Lee, J. Electron. Mater. **40**, 1321 (2011).
[13] W.J. Qiu, S.H. Yang, T.J. Zhu, J. Xie, X.B. Zhao, J. Electronic Mater. **40** (7), 1506 (2011).

[14**]** C. Schumacher, K.G. Reinsberg, L. Akinsinde, S. Zastrow, S. Heiderich, W. Toellner, G. Rampelberg, C. Detavernier, J.A.C. Broekaert, K. Nielsch, J. Bachmann, Adv. Energy Mater. **2**(3), 345 (2012).
[15] J.L. Lensch-Falk, D. Banga, P.E. Hopkins, D.B. Robinson, V. Stavila, P.A. Sharma, D.L. Medlin, Thin Solid Films **520**, 6109 (2012).
[16**]** D.A. Habboush, R.A. Osteryoung, Inorg. Chem. **23**, 1726 (1984).
[17**]** M. Lipsztajn, R.A. Osteryoung, Inorg. Chem. **24**, 3492 (1985).
[18] M.H. Yang, I.W. Sun, J. Appl. Electrochem. **33**, 1077 (2003).
[19] H. Ebe, M. Ueda, T. Ohtsuka, Electrochim. Acta **53**, 100 (2007).
[20] H. Ohno, Electrochemical aspects of ionic liquids, J. Wiley & Sons, Hoboken, N.J., 2005; 2nd edition, 2011
[21] H. P. Nguyen, X. Peng, G. Murugan, R. J. Vullers, P. M. Vereecken, J. Fransaer, J. Electrochem. Soc. **160** (2), D75 (2012).
[22] O. Mann, G.B. Pan, W. Freyland, Electrochim. Acta **54**, 2487 (2009).
[23] A.P. Abbott, G. Capper, D.L. Davies, R.K. Rasheed, V. Tambyrajah, Chem. Commun. 2003, p. 70.
[24] F. Golgovici, A. Cojocaru, C. Agapescu, Y. Jin, M. Nedelcu, W. Wang, T. Visan, Studia Univ. Babes-Bolyai, Chemia **54** (Spec. Issue 1), 175 (2009).
[25] F. Golgovici, A. Cojocaru, M. Nedelcu, T. Visan, Chalcog. Lett. **6** (8), 323 (2009).
[26] F. Golgovici, A. Cojocaru, M. Nedelcu, T. Visan, J. Electron. Mater. **39** (9), 2079 (2010).
[27] F. Golgovici, A. Cojocaru, L. Anicai, T. Visan, Mater. Chem. Phys. **126** (3), 700 (2011).
[28] F. Golgovici, T. Visan, Chalcog. Letters, 9 (10) (2012) 427-434
[29] C. Agapescu, A. Cojocaru, A. Cotarta, T. Visan, Chalcog. Lett., **9** (10), 403 (2012).
[30] C. Agapescu, A. Cojocaru, A. Cotarta, T. Visan, J. Appl. Electrochem, **43** (3) , 309 (2013).
[31] F. Golgovici, T. Visan, Chalcog. Lett. **8**, 487 (2011).
[32] F. Golgovici, T. Visan, Chalcog. Lett. **9** (4), 165 (2012).
[33] O. Ciocirlan, O. Iulian, O. Croitoru, Rev. Chim. (Bucharest) **61** (8), 721 (2010).
[34] Y. Liftman, M. Albeck, J.M.E. Goldschmidt, Ch. Yarnitsky, Electrochim. Acta **29** (12), 1673 (1984)
[35] A.S. Fouda, H.A. Mostafa, M.N. Moussa, S.M. El-Masry, J. Radioanal. Nucl. Chem. Lett. **118** (1), 45 (1987)
[36] M. Ueda, Y. Mito, T. Ohtsuka, Molten Salt, Mater. Trans. **49** (8), 1720 (2008)